



Time of flight detectors with SiPMT array readout

M. Bonesini^{a,*}, R. Bertoni^a, A. de Bari^b, R. Nardò^b, M. Prata^b, M. Rossella^b

^aSezione INFN Milano Bicocca, Piazza Scienza 3, Milano, Italy

^bDipartimento di Fisica and Sezione INFN, via A Bassi 6, Pavia, Italy

Abstract

Time-of-flight detectors, based on scintillation counters, may use conventional photomultipliers for the readout. Problems arise in presence of external magnetic fields. SiPMT arrays are insensitive to magnetic fields and may be a suitable option to replace photomultipliers. Timing performances for several types of SiPMT arrays have been studied and results are presented.

1. Introduction

Time-of-flight (TOF) detectors, based on scintillator slabs, may be assembled by using individual counters arranged in a suitable geometry, along one or two orthogonal axis. In each scintillator counter, photodetector signals may be read out at one or both ends, for redundancy, and then pulse-height analyzed. Arrival times are transformed into standard logic levels with a discriminator (constant fraction or leading edge) and then used as a STOP for a TDC, while the START signal is given from a reference counter.

A common choice for the readout devices are photomultipliers (PMTs). They may have small transit time spreads (TTS) (150–400 ps), fast risetimes (down to less than 1 ns) and large active areas. As a drawback, they are powered by high voltages (1000–2000 V) and may be sensitive to external magnetic fields. Examples of recent fast time-of-flight counters with photomultiplier readout are the large TOFW wall of the Harp experiment at CERN PS [1] with Phillips XP2020 PMTs, the TOF system of the MICE experiment at RAL [2] where conventional Hamamatsu R4998 PMTs were used [3] and the timing counter of the MEG experiment at PSI [4], [5] with fine-mesh Hamamatsu R5924 PMTs [6].

The intrinsic time resolution of a TOF detector may be parametrized as:

$$\sigma_t = \sqrt{\frac{\sigma_{sci}^2 + \sigma_{ph}^2 + \sigma_{pl}^2}{N_{pe}}} + \sigma_{elec}^2 \quad (1)$$

where: σ_{sci} accounts for the scintillator response, σ_{ph} for the photodetector jitter, σ_{pl} for the path lengths variations and σ_{elec} for the jitter of the electronic readout system. N_{pe} is the average number of photoelectrons. The separation power between two particle species (1 and 2) at a given momentum p , is given in standard deviation units by:

$$n_{\sigma_{1,2}} = \frac{L \cdot (m_1^2 - m_2^2)}{2 \cdot p^2 \cdot c \cdot \sigma_t} \quad (2)$$

and is dominated by the length L between the two TOF stations and their intrinsic resolutions σ_t . The dominating factors for σ_t are N_{pe} and the counter dimensions (mainly its length L). For resolutions below 100 ps, contributions such as σ_{ph} become increasingly important.

In the following, the question if the readout with conventional photomultipliers may be replaced by silicon photomultiplier (SiPMT) arrays, using the MICE TOF system as a benchmark ¹ has been addressed.

*corresponding author

¹no attempt was made to optimize light-guides or other detector mechanics aspect

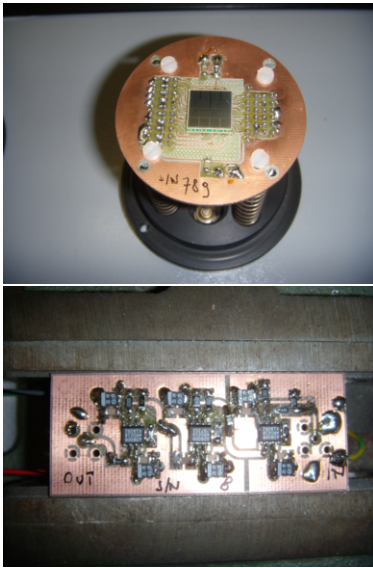


Figure 1: Top panel: image of the home-made PCB base. Bottom panel: image of the home-made amplifier.

Tests were done in laboratory with $600 \times 60 \text{ mm}^2$, 1" thick Bicron BC404 counters equivalent to the ones used for the MICE TOF2 detector [7].

2. SiPMT Array readout

SiPMT arrays from SenSL, Advansid and Hamamatsu, under test, are standard 4×4 arrays made of $3 \times 3 \text{ mm}^2$ individual SiPMT with $50 \mu\text{m}$ cell size and their main characteristics are shown in table 1.

The emission peak of the used Bicron BC-404 scintillator is around 408 nm, best suited to the NUV extended Hamamatsu or SenSL SB SiPMT arrays, as we will see later.

In the following tests, the individual SiPMT of each array are connected in parallel on a home-made PCB board (see figure 1 for details), giving a single analogue output². The output is then fed into a custom made inverting amplifier (also shown in figure 1), with pole zero suppression. The input dynamic range is between 0 and 70 mV, the amplification factor is in the range 20-35 X (according to the level of pole zero compensation) and the bandwidth is around 600 MHz. Its linearity is shown in figure 2. In some tests, commercially available amplifiers such the Phillips Scientific PLS774³ or

²this choice increases the output signal risetime, as the single SiPMT capacities are summed in the time constant of the circuit

³this module has a gain of 50-100X, a bandwidth of $\sim 1.35 \text{ MHz}$ (with inverting Pulse Transformer Phillips Scientific 460)

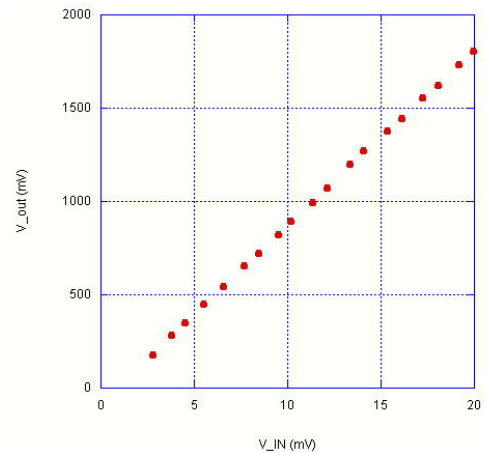


Figure 2: Linearity of the home-made amplifier.

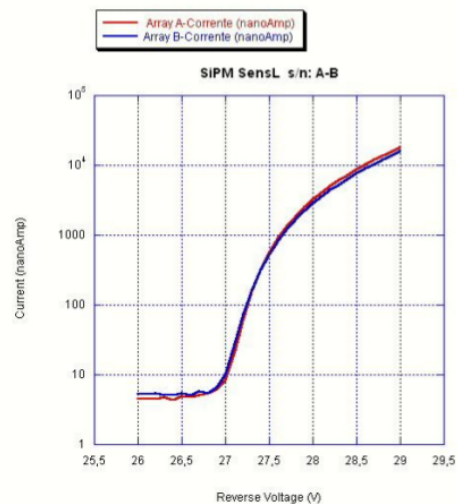


Figure 3: I-V curves for the SenSL SM-4-3035-CER arrays

the CAEN A1423⁴, with an additional circuit for pole zero suppression, were used. These modules have an increased bandwidth as respect to the used home-made amplifiers. The SiPMT arrays breakdown voltages were computed by measuring their I-V curves, using a Keithley 2600 sourcemeter⁵. An example of one I-V curve is shown in figure 2. The timing characteristics of the SiPMT arrays used for the readout of the scintillation BC404 test counter (signal risetime/falltime) have been studied with a Lecroy MX104B wideband scope. As

⁴with $\sim 1.5 \text{ GHz}$ bandwidth and variable gain between 15 dB and 50 dB

⁵with 0.02% accuracy on the set voltages and 0.03% accuracy on the measured currents

Table 1: Main characteristics of used SiPMT arrays.

	$V_{brk}(V)$	Bias range (over V_{brk})	$\lambda_{max}(nm)$	PDE (at λ_{max})
Hamamatsu S11828-3344	65 ± 10	1-4	440	$\sim 35\%$
SenSLArray SM-4-3035-CER	27.5 ± 0.5	1-5	500	$\sim 20\%$
SenSLArray SB-4-3035-CER	24.5 ± 0.5	1-5	420	$\sim 41\%$
Advansid ASD-SiPM3S-4x4A	35 ± 7	2-7	480	$\sim 22\%$
Hamamatsu S12642-50-PA (TSV)	65 ± 10	1-4	450	$\sim 35\%$

SenSL arrays have much larger values for risetimes and falltimes (at least a factor 2x), we concentrated our efforts on Hamamatsu and Advansid arrays.

3. Laboratory test setup

Timing properties of SiPMTs are commonly tested with fast diode lasers (30-50 ps FWHM) studying the single p.e. response as in [8]. To test the response of a TOF detector in realistic conditions, one has to provide instead a multiphoton signal ($\sim 200 - 300$ p.e.) with a 1-2 ns risetime, to simulate the scintillator response. We have tried to set up a system to realize these conditions. Figure 4 shows the laboratory setup used for these tests. Light is emitted from a Nichia NDHV310APC violet laser diode, driven by an Avtech fast pulser⁶ and is sent, via a 1m multimode fiber⁷, to the scintillation counter injection system (made of a total reflection prism). The laser spot is focused into the optical fiber (aligned by a micrometric x-y-z 3-stages system⁸) by a 10x Newport microscope objective. Light signals of different intensities were obtained both by tuning the laser parameters (e.g. amplitude and pulse width) and by changing the beam focussing onto the injection system. The laser beam is splitted by a broadband beamsplitter (BS) to give 50% of light on the fiber injection system and 50% on a monitoring detector. A fast Thorlabs DET10A/M photodiode (risetime ~ 1 ns) is used to monitor the laser intensity and give a reference start signal (t_0) for the TDC system. The reference photodiode signal is amplified by a wideband CAEN A1423 inverting amplifier. Four timing signals (t_0, t_s, t_1, t_2) are then recorded by the acquisition system. t_1, t_2 refer to the two photodetectors

at the edge of the scintillation counter, while t_0 refers to the reference photodiode output and t_s to the laser driver sync-out.

The acquisition system is based on a VME-PCI interface card (CAEN V2718) and data, written as binary files, are then analyzed via the ROOT package [10]. The two signals: t_1, t_2 from the edges of the scintillation counter under test, are splitted (50% – 50%) by SUHNER passive splitters. They are sent to both a QADC line (CAEN V792) and a TDC line (with a CAEN V1290 TDC module after a CAEN V895 leading edge discriminator). Care has been taken to have comparable signals at both L/R photodetectors, to avoid sizeable time-walk corrections.

In some measurements, the VME DAQ system was replaced by an ORTEC TAC/SCA 567 and a CAEN N957 8K MCA. The TAC was calibrated with delay cables of known length.

The signal from the laser system was tuned in pulse amplitude and width to obtain a timing resolution for a counter equipped with two Hamamatsu R4998 PMTs, equivalent to the one obtained in a previous BTF testbeam at LNF, Frascati, for the same type of counters [2]. From the gaussian fit of the Δt_- distribution⁹ of figure 5 a resolution of ~ 43 ps is obtained, to be compared with a value of ~ 45 ps, obtained at the LNF BTF testbeam¹⁰. This result established the conditions for the use of the laser system in the following tests. In figure 6 the intrinsic counter resolution $\sigma_t = \sigma_{\Delta t_-}/2$ is reported as a function of the PMTs operating voltage $V_{op} = V_0 + \Delta V$. In normal operating conditions resolutions $\sigma_t \sim 40$ ps are obtained.

4. Experimental results

With the same laser beam tuning, data were taken with the SiPMT arrays in place of the R4998 photomul-

⁶Avtech AVO-9A-C laser diode driver, with ~ 200 ps risetime and a AVX-S1 output module. This system gave laser pulses at ~ 408 nm, with a pulse length between ~ 400 ps and ~ 3 ns (as measured with a 6 GHz 6604B TEK scope) and repetition rate up to 1 MHz

⁷CERAM OPTEC UV 100/125 optical fiber, with a measured dispersion of ≤ 15 ps/m, see [9]

⁸Thorlabs MBT613/M with a 4 mm excursion and $\sim 0.5\mu m$ resolution

⁹ Δt_- is defined as the difference of the discriminated time signal from the two counter edges. The intrinsic TOF detector resolution may be then computed as $\sigma_t = \sigma_{\Delta t_-}/2$

¹⁰with data taken with impinging electrons giving a 2-3 MIP signal

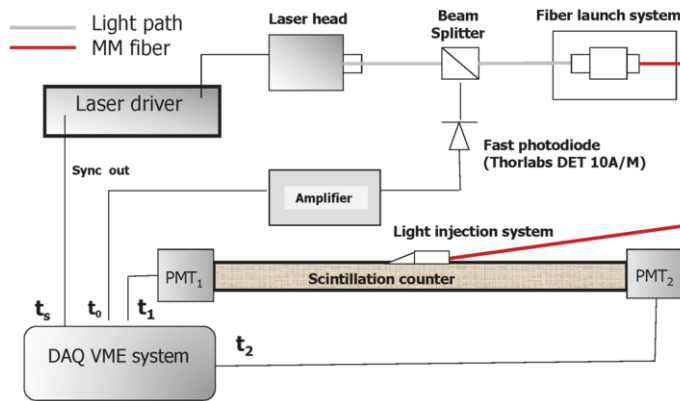


Figure 4: Laboratory test setup used in the photomultipliers and SiPMT arrays readout characterization.

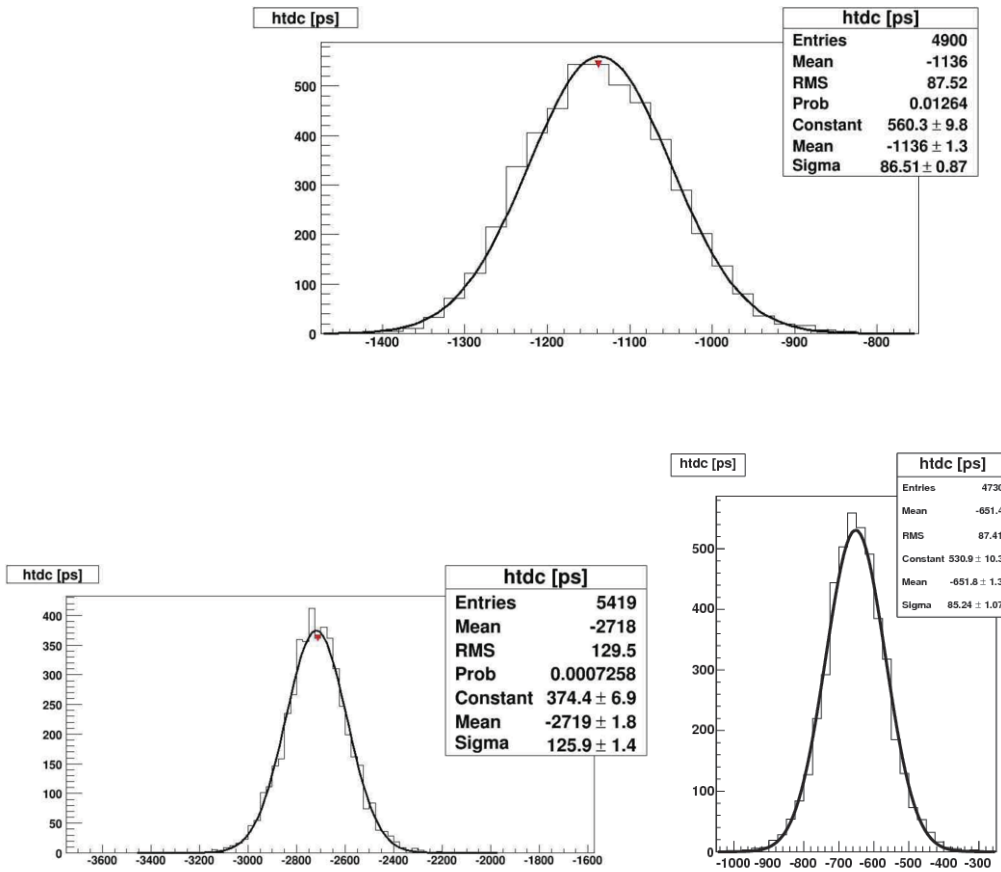


Figure 5: Top panel: distribution of Δt_{-} for the counter under test, equipped with R4998 PMTs at the two extremes. A gaussian fit is superimposed. Standard HV settings are used for both PMTs (-1750 V, -2250 V). Bottom panels: same distributions for the counter under test, equipped instead with Hamamatsu S1182-3344 arrays, operating voltage is 72.5 V (right) and Advansid ASD-SiPM3S-4x4A arrays, operating voltage is 33.4 V (left).

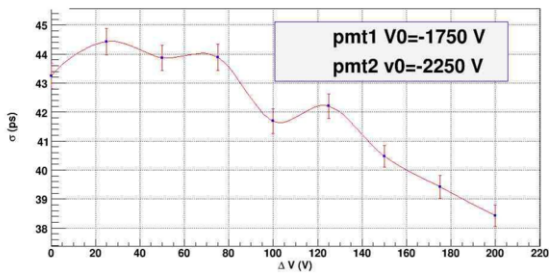


Figure 6: Intrinsic time resolution σ_t for the counter under test equipped with conventional Hamamatsu R4998 PMTs

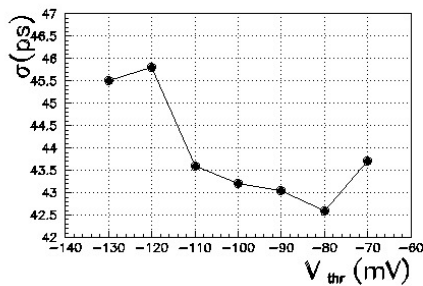


Figure 7: Intrinsic time resolution σ_t at fixed voltages V_{op} obtained for the scintillation counter under test, equipped with Hamamatsu S11828 arrays at $V_{op} = 72.5V$.

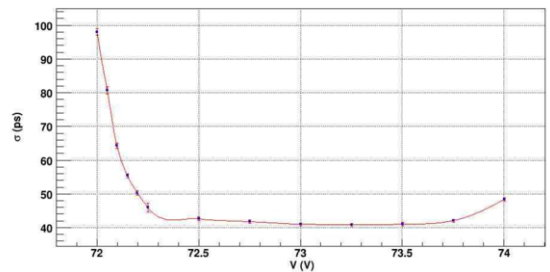
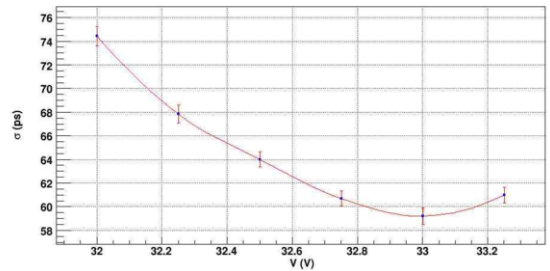


Figure 8: Intrinsic time resolution σ_t vs the operating voltage V_{op} obtained for the scintillation counter under test, equipped with Hamamatsu S11828 (bottom panel) or Advansid ASD-SiPM3S-4x4A (top panel) SiPMT arrays.

tipliers. By varying the operating voltage $V_{op} = V_{brk} +$ overvoltage a scan was done in both cases using a suitable threshold for the leading edge discriminator. The optimal value of this threshold (~ -80 mV) was chosen for the tested SiPMT arrays with scans at fixed operating voltages (see figure 7 for an example).

The best results are obtained with Hamamatsu arrays that are NUV extended, while the Advansid ones are RGB (with peak response at ~ 500 nm). Some results are shown in figure 8. For Hamamatsu S11828 arrays an intrinsic counter resolution $\sigma_t \sim 40$ ps is reached on an extended region of operating voltages, while for Advansid ASD-SiPM3S-4x4A arrays resolutions are at best ~ 60 ps.

As a limiting factor for the readout electronics of the used SiPMT arrays may be the bandwidth of the used home-made inverting amplifiers (~ 600 MHz), tests with a commercial wideband NIM amplifier: a Phillips Scientific 774 module with external circuits for pole-zero compensation¹¹ were done. Results are shown in figure 9 for the Hamamatsu SiPMT arrays. No appreciable improvements are seen.

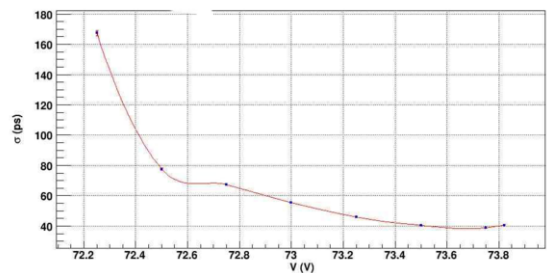


Figure 9: Intrinsic time resolution σ_t vs the operating voltage V_{op} obtained for the scintillation counter under test, equipped with Hamamatsu S11828 SiPMT arrays. A PLS774 amplifier is used.

¹¹the nominal 50X gain was thus reduced to about 13X

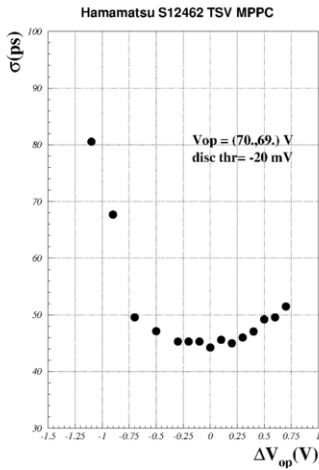


Figure 10: Intrinsic time resolution σ_t vs the operating voltage V_{op} for the scintillation counter under test, equipped with Hamamatsu S12462 SiPMT TSV arrays.

4.1. Results with 4×4 TSV arrays

The TSV (“through Silicon Via”) technology is used to avoid the need of a wire bonding pad, that creates dead spaces in the detector area. The anode of each channel is traced to the backside panel by a TSV. In principle, the timing jitter must be smaller. Tests were done on the Hamamatsu TSV S12462 arrays with only PLS 460 pulse inverters and no amplification stage. Preliminary results are shown in figure 10, where no clear improvements as respect to timing are seen as respect to more conventional SiPMTs arrays.

4.2. Rate effects for SiPMT arrays

Under an increasing particle rate, a photodetector may show fatigue effects that are seen as a non-linearity of the response or a deterioration of the time resolution. With an increasing laser frequency between 10 KHz and 1 MHz, no effects are seen for the conventional Hamamatsu R49998 PMT’s readout up to 10^5 Hz and a small one for the SiPMT arrays, as shown in figure 11.

For further studies, the burst structure of an accelerator (e.g. the one of the ISIS machine at RAL, with 50 Hz repetition rate and a burst structure with pulses of ~ 100 ns flat top, separated by ~ 230 ns) has been simulated, as shown in figure 12. Some results are shown in figure 13 and also here no clear effect is evident up to 10^5 Hz.

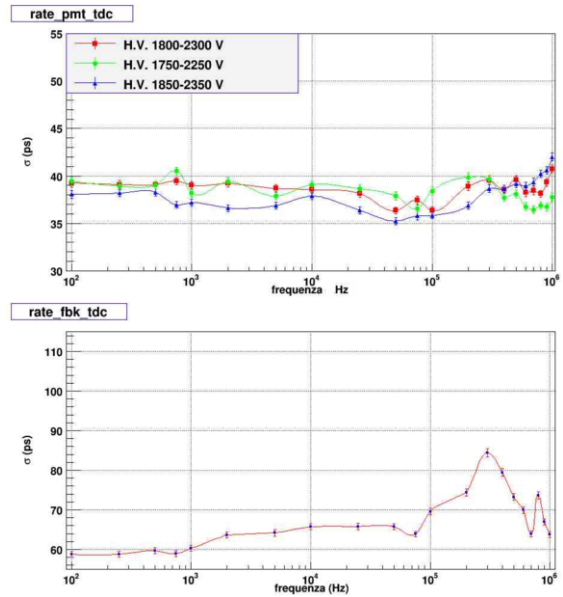


Figure 11: Intrinsic time resolution σ_t vs the laser repetition frequency for the scintillation counter under test, equipped with conventional Hamamatsu R4998 PMTs (top) or Advansid siPMT Arrays (bottom).

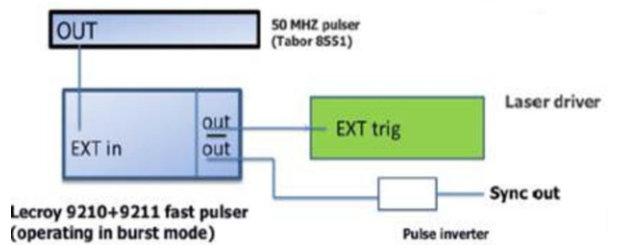


Figure 12: Layout of the system used to simulate the ISIS accelerator burst structure, giving an external trigger to the used laser system.

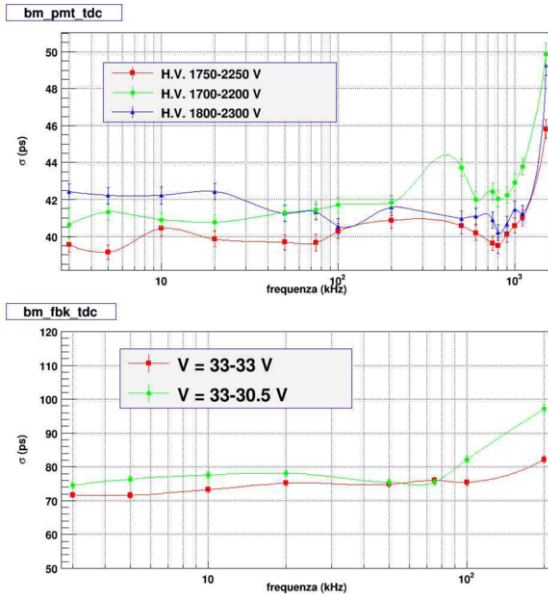


Figure 13: Intrinsic time resolution σ_t vs the laser repetition frequency for the scintillation counter under test, equipped with conventional Hamamatsu R4998 PMTs (top) or Advansid SiPMT Arrays (bottom). Tests are done simulating the burst structure of the ISIS accelerator at RAL.

Conclusions

Available SiPMT arrays are suitable readout devices for time-of-flight detectors based on scintillation counters. Timing resolutions σ_t , comparable with the best values obtained with photomultipliers, may be obtained by using a proper operating voltage. NUV extended Hamamatsu SiPMT arrays show better performances, as compared to RGB types as Advansid ASD-SiPM3S-4x4A, for conventional scintillator readout.

Rate effects for SiPMT arrays are of the same size as the one experienced by conventional photomultipliers with active dividers.

Acknowledgments

We would like to acknowledge the skilfull work of Mr. R. Mazza, F. Chignoli INFN Milano Bicocca and Mr. D. Calabró, A. Freddi, C. Scagliotti, F. Vercellati INFN Pavia for the realization of the test setup and the relative mechanics and electronics. We would like to thanks Dr. N. Serra (Advansid), C. Piemonte (FBK/IRST) and M. Bombonati (Hamamatsu) for fruitful discussions and technical advice. We acknowledge also the essential work of our students L. Maver and G. Stringhini who took part with dedication and enthusiasm in the reported measurements.

References

- [1] M. Baldo-Ceolin et al., *The time-of-flight TOFW detector of the HARP experiment: construction and performance*, *Nucl. Instr. Meth. A* **532** (2004) 548
- [2] R. Bertoni et al., *The design and commissioning of the MICE upstream time-of-flight system*, *Nucl. Instr. and Meth. A* **615** (2010) 14.
- [3] M. Bonesini et al., *Behaviour in Magnetic Fields of Fast Conventional and Fine-Mesh Photomultipliers*, *Nucl. Instr. and Meth. A* **693** (2012) 130.
- [4] A. De Gerone et al., *The MEG timing counter calibration and performance*, *Nucl. Instr. Meth. A* **638** (2011)41
- [5] S. Dussoni et al., *The Timing Counter of the MEG experiment: Design and commissioning*, *Nucl. Instr. Meth. A* **617** (2010) 387
- [6] M. Bonesini et al., *Behaviour in high magnetic fields of fine-mesh photodetectors for fast time-of-flight detectors*, *Nucl. Instr. Meth. A* **567** (2006) 200
- [7] R. Bertoni et al., *The construction of the TOF2 detector*, MICE-NOTE-DET-0286, 2010.
M. Bogomilov et al. [MICE Coll], *The MICE Muon Beam on ISIS and the beam-line instrumentation of the Muon Ionization Cooling Experiment*, JINST 7(2012) P05009.
- [8] V. Puill et al., *Single photoelectron timing resolution of SiPM as a function of the bias voltage, the wavelength and the temperature*, *Nucl. Instr. Meth. A* **695** (2012) 354
- [9] M. Bonesini et al., *Laser-based Calibration for the HARP Time of Flight System*, *IEEE Trans. Nucl. Sc.* **NS-50** (4) (2003) 1053.
- [10] [Http://root.cern.ch](http://root.cern.ch)